Proceedings of the Korean Nuclear Society Autumn Meeting
Seoul, Korea, October 1998

Effect of Intercritical Annealing Treatment on the Mechanical Properties of SA106 Gr.C Piping Steel

Joo Suk Lee, In Sup Kim

Korea Advanced Institute of Science and Technology
373-1, Kusong-dong, Yusong-gu, Taejon 305-701, South Korea

Abstract

It is reported that SA106 Gr.C piping steel generally exhibits not enough toughness to apply LBB concept and needs a suitable additional heat treatment to improve the toughness. The intercritical annealing at the ($\alpha+\gamma$) phase temperature at 760°C for 40 min was performed in this study. To evaluate the improved material properties with the heat treatments, tensile tests were carried out under various temperatures, from RT to 350°C, and strain rates, from $1.39x10^{-4}s^{-1}$ to $1.39x10^{-2}s^{-1}$. Also, Charpy impact tests were conducted to measure impact toughness at room temperature. The manifestations of dynamic strain aging (DSA) were observed in the tensile properties. However, the magnitude of serration and the strength increased by DSA was relatively small compared to similar grade carbon steels. The intercritical annealing was able to increase the impact toughness by 1.5 times compared to as-received material. The dissolved carbon content in the retained ferrite, which was formed at the ($\alpha+\gamma$) region, may be lower than that in the transformed ferrite, which was formed at the pearlite transformation temperature. It is considered that the cleaner retained ferrite may have caused the higher impact toughness and ductility in addition to the general toughening due to finer grain sizes, which were resulted from the heat treatment.

I. Introduction

The SA106 Gr.C piping steel, which was selected for Korea Next Generation Reactor (KNGR) and already used in PWR main steam line piping, showed a substantial reduction in toughness due to dynamic strain aging (DSA) at the reactor operating temperature [1]. From this point, the Leak-Before-Break (LBB) concept has been difficult to apply to the main steam line piping.

The physical manifestations of DSA in steels are serrated flow curves, high work hardening rates, negative or zero strain rate sensitivity, pronounced strengthening and reduction of ductility. The DSA in steels is the result of simultaneous interactions between dislocations and dissolved carbon and nitrogen atoms in the ferrite matrix during the straining [2]. Because the amount of dissolved nitrogen or carbon for DSA is extremely small even less than 0.0001% [3], complete elimination of DSA in carbon steel is difficult, yet, it is possible to control degree of DSA by adding alloying elements or by heat treatment [3].

The ferrite matrix, which was formed at normal air cooling after hot extrusion, has relatively high carbon content because of high cooling rate from the austenite at the working temperature. An additional heat treatment, namely, intercitical annealing, was introduced to obtain cleaner ferrite matrix and finer grain size.

The dissolved carbon content in the retained ferrite (old-ferrite), which was formed at the ($\alpha+\gamma$) region, has been known to be lower than that in the transformed ferrite (new-ferrite), which was formed at the pearlite transformation temperature [4].

The purposes of this study are to improve toughness and to reduce DSA susceptibility for the LBB applicability of SA106 Gr.C main steam line piping.

II. Experimental Procedure

Material Preparation

The SA106 Gr.C carbon steel used in this study was received from Hanjung, which was the archive material of main steam line piping of Young Gwang Units 3 and 4 which have dimensions of 669mm outer diameter and 28.6 mm thickness. The chemical composition is given in Table I and the microstructure was a typical ferrite-pearlite band structure.

Heat Treatments

As-received SA106 Gr.C, which was normalized after hot extrusion of the seamless piping, was homogenized in the austenite range at 950°C for 1hr in a vacuum furnace and furnace cooled (F). Then the F specimens were annealed in the ferrite plus austenite phase field at 760°C. After a holding time of 40 min, the specimens were subjected to either air (FA) or furnace cooled (FF). The cooling rates from 760°C for the FF and FA were approximately 0.02°C/s and 0.5°C /s respectively.

Table 1. Chemical composition of SA106 Gr.C (w/o)

C	Mn	P	S	Si	Ni	Cr	Mo	V	Al	Cu	H ppm
0.19	1.22	0.009	0.007	0.27	0.11	0.05	0.03	0.004	0.029	0.13	1.6

Mechanical Testing and Microscopy

The tensile specimens were machined with an 8mm diameter and 40mm gage lengths, such that their tensile axis was parallel with pipe axis (L-direction). Standard Charpy V-notch impact specimens were machined by the ASTM E-23 and tested at room temperature. Charpy impact specimens were in the L-C direction. Tensile tests were carried out at various temperatures, from RT to 350°C, and at strain rates, from $1.39x10^{-4}$ to $1.39x10^{-2}$ s^{-1}. Specimen temperature was measured by thermocouples, which were welded at upper and lower parts in the specimen, and strain was measured by the 0.1 in (0.254cm) extensometer. Tests were performed at universal testing machine (AG-10TA of Shimadzu). Nital (2% nitric acid + 98% ethanol) and boiling alkaline chromate solution (8g CrO_3 + 40g NaOH + 72*ml* pure water) etching [5] revealed the microstructures composed of a pearlite and both kinds of ferrite, namely, retained and transformed.

III. Results and Discussion

Microstructures

Fig.1 (a), (b) and (c) illustrate the optical microstructures developed by the heat treatments F, FA and FF, respectively. Fig.1 (a) shows typical ferrite-pearlite band structure, which was caused by the interdendritic segregation of Mn during solidification [6]. Fig.1 (b) and (c) show the air (FA) and furnace cooled (FF) microstructures after the intercritical annealing. The FA specimen has a narrower pearlite band spacing than the F and FF specimens have. It is considered that the FA condition did not give enough time for carbon atoms to diffuse in the austenite phase during air cooling and resulted in narrower pearlite band. On the other hands, FF condition allowed enough time for carbon atoms to diffuse in the austenite during furnace cooling and resulted in a dispersed perlite band. This is clearly observed in low magnification optical microscopy in Fig.2 (a), (b) and (c).

Fig.3 shows para-equilibrium (carbon equilibrium) ferrite-austenite (martensite) phase at 760°C. This figure shows that austenite phase grows in pearlite and along ferrite grain boundary because austenite growth needed high carbon content and easy diffusion path along the grain boundary.

To distinguish between retained and transformed ferrite, boiling alkaline chromate solution etching [5] was conducted to the specimen FA and FF. The results are in Fig.4 (a) and (b), (white = transformed ferrite, gray = retained ferrite, black = pearlite)

From the observation of Fig.4 (a) and (b) there is no grain boundary between transformed and retained ferrite. It has been suggested that on cooling after the intercritical annealing the transformed ferrite grows epitaxially on the retained ferrite [7]

Tensile tests

Tensile tests were conducted at three different strain rates and various temperatures to understand the DSA phenomena in F, FA and FF specimens.

Fig.5 (a), (b) and (c) show the effects of temperature on stress-strain curves at a strain rate (SR) of $1.39x10^{-3}$ s^{-1} of heat-treated specimens. In the stress strain curves, the serrated flow behavior has been observed at a certain combination of temperature and strain rate, but the stress amplitude in serrated flow was relatively small. Other stress-strain curves with different strain rates are not presented because there was no deviation from the established trend. Increasing temperature has the same effect as reducing strain rate on DSA.

Fig.6 (a), (b) and (c) represent the variation in ultimate tensile stress (UTS) and yield stress (YS) of heat-treated materials with at different temperatures and strain rates. UTS and YS varied with temperature, the peak of UTS occurred around 290°C and moved to higher temperature with increasing strain rate. At RT and 350°C, UTS showed a positive strain rate sensitivity, but at the intermediate temperature range, negative strain rate sensitivity was observed, which is one of the DSA characteristics (Baird, 1971). YS gradually decreased with increasing temperature, but in the UTS peak temperature range there appeared plateau or somewhat increased yield stress.

The effects of testing temperature at three different strain rates on the total (TE) and uniform (UE) elongation are shown in Fig.7 (a) and (b) on the F and FA specimens. With increasing temperature, the total elongation decreased up to the temperature region of UTS peak and then increased at higher temperature at all heat-treated conditions. However, uniform elongation somewhat increased or remained at the similar level of room temperature test results.

To investigate the effects of intercritical annealing treatment, TE and UE were compared for the same strain rate, $1.39x10^{-3}$, on each heat-treated specimen. Fig. 8 shows change in elongation at various temperatures.

At room temperature, FF specimen shows a higher ductility than the others. However, as the test temperature increased, FF resulted in the same elongation as the FA condition, but both FF and FA conditions had a higher ductility than the F condition, which was not intercritical annealed, at the reactor operating temperature.

It could be explained by the facts that soft retained ferrite and dispersed pearlite band by the intercritical annealing gave higher ductility than the F condition. From the Fe-C phase diagram, it is evident that the carbon content in the retained ferrite, which was formed at the ($\alpha+\gamma$) region, may be lower than that the transformed ferrite, which was formed at lower temperature [4].

Charpy impact tests

To investigate improved the impact toughness by the additional heat treatment, standard Charpy V-notch (CVN) impact tests were performed at room temperature. Fig.9 showed the test results. From the test results, the furnace cooled specimens after intercritical annealing (FF) had higher toughness by 1.5 times as compared to as-received material. It could be explained that the clean retained ferrite may have caused the higher impact toughness and ductility in addition to the general toughening due to somewhat finer grain sizes, which were resulted from the intercritical annealing treatment, the trends are agreement with tensile test results at room temperature.

III. Conclusions

1. After intercritical annealing treatment, we could obtain both kinds of ferrite, retained and transformed. Furnace cooled specimens after intercritical annealing shows more ferrite content and dispersed pearlite band than that in the air cooled specimens.
2. In all heat treatments, dynamic strain aging in SA106 Gr.C was observed in tensile properties. However, the magnitude of serration and the strength increased by DSA were relatively small compared to similar grade carbon steels
3. Either air or furnace cooled specimens after intercritical annealing, total elongation at a strain rate of $1.39x10^{-3}s^{-1}$ was increased compared to the furnace cooled specimens after austenizing at the reactor operating temperature.
4. The furnace cooled after intercritical annealing showed about 50% increase in the impact toughness compared to as-received material.

References

1. Jin Weon Kim, In sup Kim, *Nuclear Engineering and Design*, vol.172, 1997, p 49~59.
2. J. D. Baird, *Metallugical Reviews*, vol. 16, 1971, p1.
3. W. C. Lesile and R. L. Rickett, *Trans. of AIME*, Aug.1983, p1021.
4. Joon Jeong Yi, In Sup Kim, *Scripta METALLURGICA*, vol. 17, P299~302. 1983
5. R. D. Lawson, D. K. Matlock, and G. Krauss, *Metallography*, vol. 13, p 71, 1980.
6. William C. Leslie, *the physical metallurgy of steels*, p 172~177.
7. Matlock, D. K., Krauss, G., Ramos, L. F., and Huppi, G. S., *Structure and Properties of Dual-Phase Steels*, PP. 62~90. AIME, New York, NY, 1979

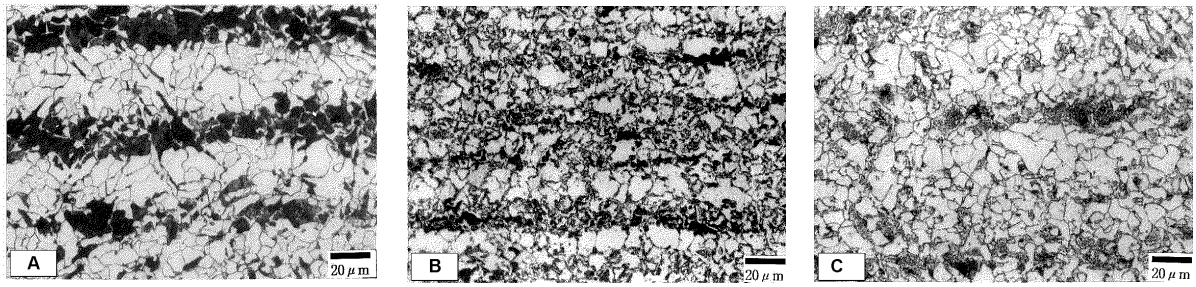

Fig. 1 The microstructures on each heat-treated conditions in SA106. Gr.C. (a) F, (b) FA and (c) FF specimens. Black = pearlite, White = ferrite.

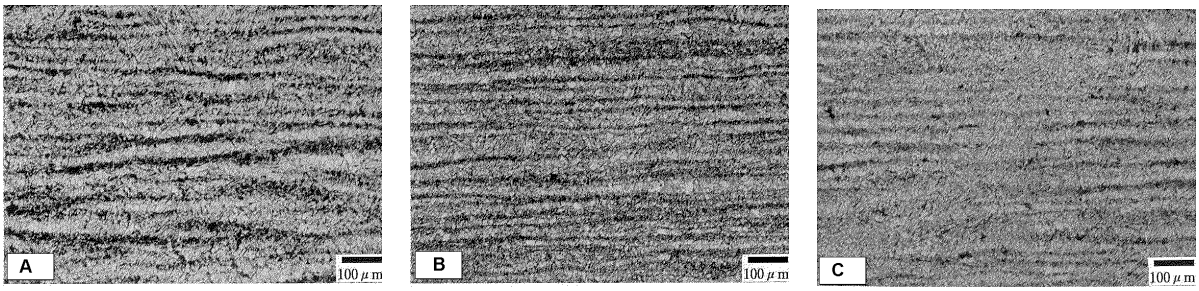

Fig. 2 Low magnification of the optical microscopy in SA106 Gr. C. (a) F, (b) FA and (c) FF specimens. Black = pearlite, White = ferrite.

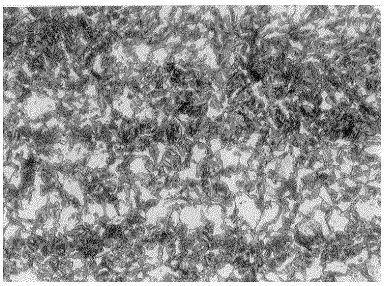

Fig. 3 The microstructure after water quenching from the intercritical annealing at 760 °C for 40min. White = ferrite, Black = martensite

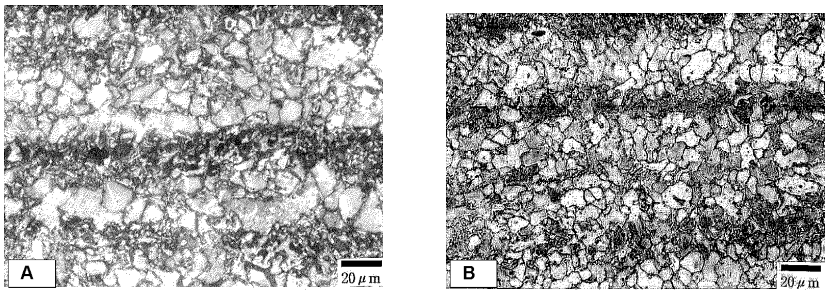

Fig. 4 The microstructures of FA and FF conditions. (a) FA (b) FF specimens. Boiling alkaline chromate solution etched. Black = pearlite, white = transformed ferrite, gray = retained ferrite.

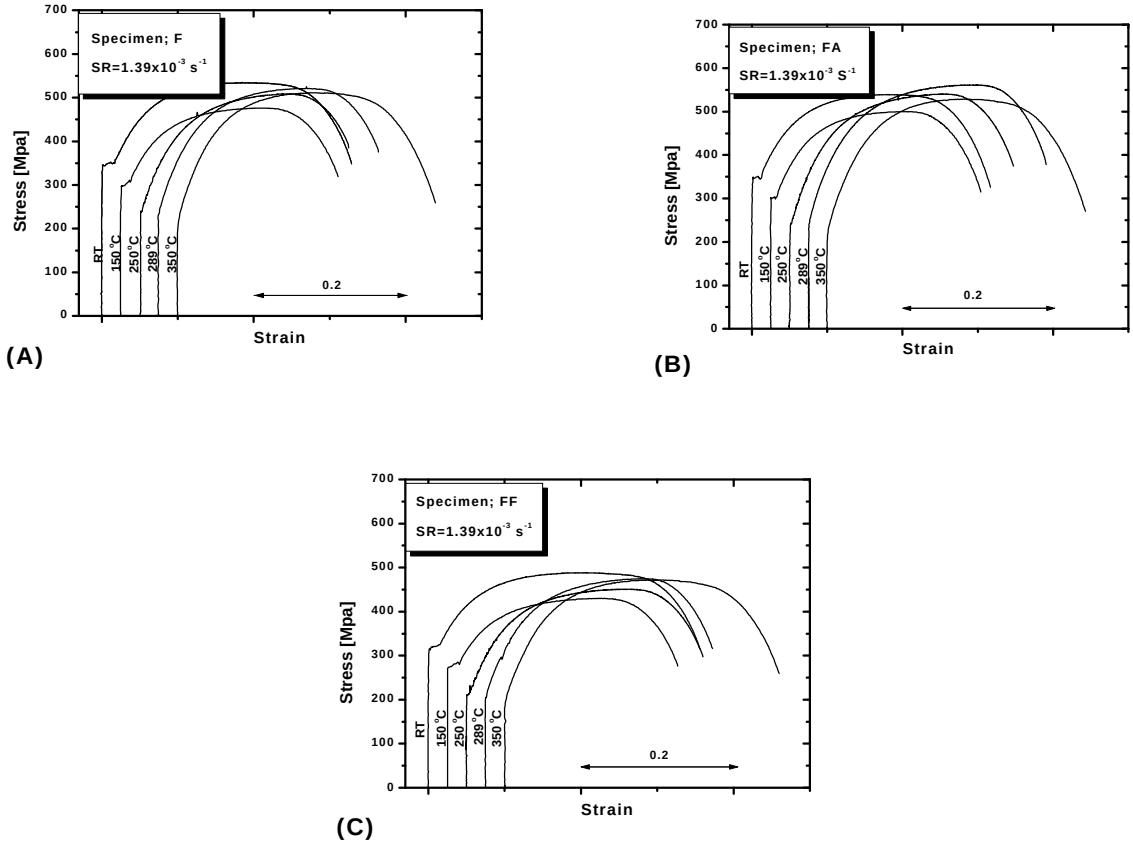

Fig.5 Stress-strain curves at various temperatures at a strain rate of $1.39x10^{-3}$ s^{-1} of heat-treated specimens. (a) F, (b) FA and (c) FF.

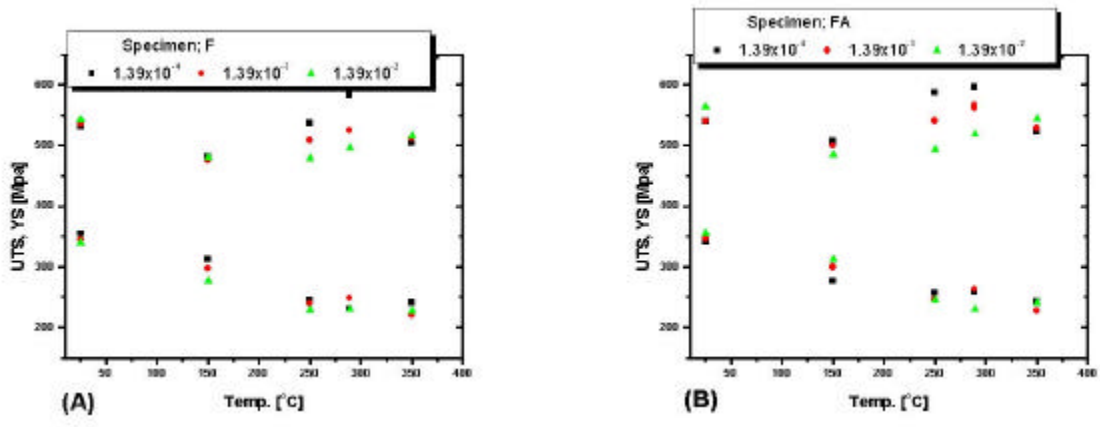

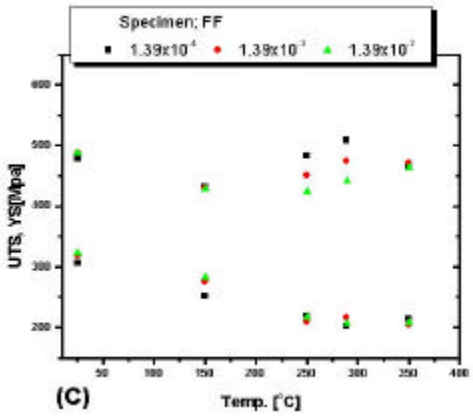

Fig.6 Dependence of UTS and YS with temperatures and strain rates of heat-treated specimens. (a) F, (b) FA and (c) FF.

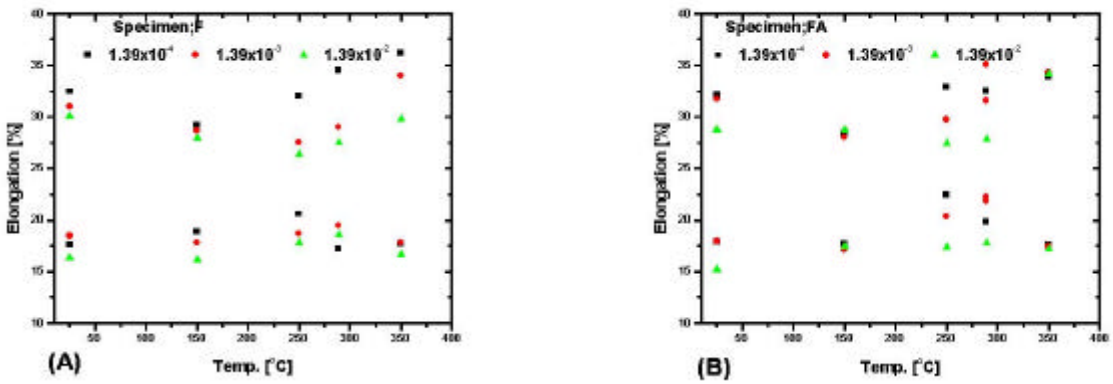

Fig.7 Variation of total and uniform elongation with temperatures and strain rates. (a) F and (b) FA.

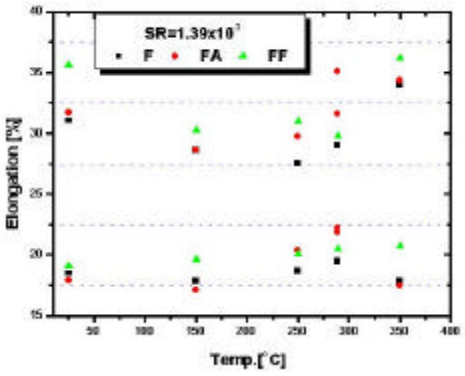

Fig. 8 Total and uniform elongation at various temperatures of heat-treated sprecimens at a strain rate of $1.39x10^{-3}$ s^{-1}.

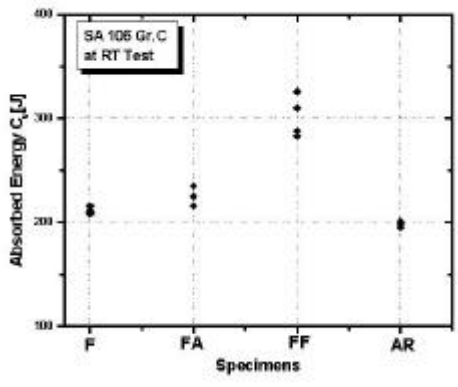

Fig. 9 Charpy impact test at room temperature of heat-treated specimens.